Journal of Bone and Mineral Metabolism (2019) 37:235–242
https://doi.org/10.1007/s00774-018-0927-y

ORIGINAL ARTICLE

Establishment and characterization of a C57BL/6 mouse model of bone metastasis of breast cancer

Toru Hiraga[1] · **Tadashi Ninomiya**[2,3]

Received: 29 January 2018 / Accepted: 2 April 2018 / Published online: 17 April 2018

Abstract

Bone is one of the most common sites of metastasis in patients with advanced breast cancer; however, the mechanisms of bone metastasis remain to be fully elucidated. Animal models are essential research tools for investigating the mechanisms of diseases and drug actions. To date, there have only been a few reports in which C57BL/6 mice were used for the study of bone metastases of breast cancer. In the current study, we found that intracardiac inoculation of C57BL/6 mouse-derived parental E0771 breast cancer cells (E0771/Pa) frequently lead to bone metastases in C57BL/6 mice within 2 weeks. The bone-metastatic clone of E0771 (E0771/Bone) established by sequential in vivo selection demonstrated a higher bone-metastatic potential. Although there were no apparent differences in cell morphology or proliferation in monolayer cultures, E0771/Bone showed increased tumorsphere formation in suspension cultures and tumor formation in the orthotopic mammary fat pad in C57BL/6 mice compared with E0771/Pa. Furthermore, E0771/Bone expressed breast cancer stem-like cell surface markers $CD24^{-}/CD44^{+}$. These findings suggest that E0771/Bone possesses cancer stem-like properties. Quantitative PCR analysis revealed that mRNA expression of parathyroid hormone-related protein (PTHrP), the most common mediator of osteolytic bone metastases of breast cancer, was significantly upregulated in E0771/Bone. Thus, cancer stem-like properties and elevated PTHrP expression likely contribute to the enhanced metastatic potential of E0771/Bone. We believe that this new mouse model is a useful tool for in vivo studies of bone metastases of breast cancer, especially for those using genetically engineered mice with a C57BL/6 background.

Keywords Bone metastasis · Breast cancer · Animal model · E0771 cells · C57BL/6 mouse

Introduction

Breast cancer is the most common cancer and the leading cause of cancer death among women in Japan and the United States [1, 2]. Bone is one of the most frequent sites of metastasis in patients with advanced breast cancer [3]. Bone metastases cause skeletal-related events, including bone pain, pathological fractures, spinal compression, and hypercalcemia. Consequently, bone metastases are major causes of increased morbidity and eventual mortality in breast cancer patients [3]. However, the mechanisms of bone metastases have yet to be fully elucidated.

Animal models are essential research tools for investigating the mechanisms of diseases and drug actions. C57BL/6 is the most commonly used mouse strain for the generation of transgenic and knockout mice [4]. To employ these mice for cancer study, syngeneic C57BL/6-derived cell lines, such as B16 melanoma and Lewis lung carcinoma cell lines, have been utilized [5, 6]. However, there have only been a few reports in which C57BL/6 mice were used for the study of bone metastases of breast cancer [7, 8].

E0771 is a cell line of medullary breast carcinoma that is derived from a spontaneous mammary tumor that arose in a wild-type C57BL/6 mouse [9]. Although it has been demonstrated that E0771 cells are tumorigenic in C57BL/6 mice and metastasize to the lungs spontaneously and also by intravenous inoculation [10, 11], the bone-metastatic ability of E0771 cells remains to be determined.

✉ Toru Hiraga
bone.mets@gmail.com

[1] Department of Histology and Cell Biology, Matsumoto Dental University, 1780 Gobara-Hirooka, Shiojiri, Nagano 399-0781, Japan

[2] Division of Hard Tissue Research, Institute for Oral Science, Matsumoto Dental University, Shiojiri, Nagano, Japan

[3] Department of Anatomy, Nihon University School of Dentistry, Chiyoda-ku, Tokyo, Japan

In the current study, we found that intracardiac injection of parental E0771 cells leads to bone metastases in C57BL/6 mice. Furthermore, we established a highly bone-metastatic clone of E0771 cells by repeated sequential in vivo selection [12, 13], and successfully developed a C57BL/6 mouse model of bone metastases of breast cancer.

Materials and methods

Cell cultures

The mouse breast cancer cell lines E0771 (CHs Biosystems, Buffalo, NY) and 4T1 (a generous gift from Dr. Fred R. Miller, Michigan Cancer Foundation, Detroit, MI) [14] and the human breast cancer cell line MCF-7 (American Type Culture Collection, Rockville, MD) were cultured in Dulbecco's modified Eagle's medium (Sigma-Aldrich, St. Louis, MO) supplemented with 10% fetal bovine serum (Mediatech, Manassas, VA) and 100 μg/ml kanamycin sulfate (Meiji Seika Pharma, Tokyo, Japan), and were maintained in a humidified atmosphere of 5% CO_2 in air at 37 °C.

Cell proliferation in monolayer cultures

The cells (1000 cells/well) were plated in growth medium in 96-well plates and cultured for 24, 48, and 72 h. Cell proliferation was determined using Cell Counting Kit-8 (Dojindo Laboratories, Kumamoto, Japan), in which WST-8 (2-(2-methoxy-4-nitrophenyl)-3-(4-nitrophenyl)-5-(2,4-disulfophenyl)-2H-tetrazolium) is used as a substrate, according to the manufacturer's protocol. The absorbance was measured using a microplate reader (Bio-Rad Laboratories, Hercules, CA) at a wavelength of 450 nm. Each assay was conducted in quadruplicate.

Tumorsphere formation

Tumorsphere formation was assessed as previously described [15]. After cultivation for 6 days, the number of tumorspheres with a diameter of > 200 μm was counted by light microscopy. Data are expressed as the number of tumorspheres/well. Each assay was performed in quadruplicate.

Reverse transcriptase-polymerase chain reaction (RT-PCR)

RT-PCR was performed as previously described [16]. Primer sequences were as follows: mouse estrogen receptor α (ERα; product size 221 bp), GCCAAGGAGACTCGC TACTG/TTCATCATGCCCACTTCGTA; mouse progesterone receptor (PgR; product size 159 bp), GATTCAGAA GCCAGCCAGAG/GTTATGCTGCCCTTCCATTG; mouse v-erb-b2 erythroblastic leukemia viral oncogene homolog 2 (Erbb2; product size 162 bp), GACTGTGTGGGAGCT GATGA/TCGGAGTCAATCATCCAACA; mouse parathyroid hormone-related protein (PTHrP; product size 206 bp), CAGCCGAAATCAGAGCTACC/CTCCTGTTCTCTGCG TTTCC; mouse glyceraldehyde-3-phosphate dehydrogenase (GAPDH; product size 338 bp), TTGAAGGGTGGAGCC AAACG/ACACATTGGGGGTAGGAACACG; human GAPDH (product size 415 bp), CATGGAGAAGGCTGG GGCTC/CACTGACACGTTGGCAGTGG. The primers for ERα, PgR, and Erbb2 can also amplify human genes, and the product sizes are exactly the same as those of mice. The absence of contamination of DNA was verified by PCR on non-reverse-transcribed RNAs. The sizes of the fragments were confirmed by reference to a 100-bp DNA ladder.

Real-time RT-PCR

In some experiments, cells were treated with transforming growth factor-β1 (TGFβ, 5 ng/ml, Peprotech, Rocky Hill, NJ) for 24 h. Real-time RT-PCR was performed using a One Step SYBR PrimeScript PLUS RT-PCR Kit (Takara Bio, Shiga, Japan) with a StepOnePlus Real-Time PCR system (Applied Biosystems, Foster City, CA). Primer sequences were as follows: mouse ERα, CAACTGGGCAAAGAGAGT GC/CCAGACGAGACCAATCATCA; mouse PTHrP, GGT TCAGCAGTGGAGTGTCC/CAGACACAGCGCGTTTGA; mouse B-cell-specific Moloney murine leukemia virus integration site 1 (BMI1), CAAAACCAGACCACTCCTGAA/ TCTTCTTCTCTTCATCTCATTTTTGA; mouse aldehyde dehydrogenase 1 family, member A1 (ALDH1A1), GCC ATCACTGTGTCATCTGC/CATCTTGAATCCACCGAA GG; mouse β-actin, CTAAGGCCAACCGTGAAAAG/ ACCAGAGGCATACAGGGACA. Melting curve analysis was performed to determine the melting temperatures of the amplified products and exclude undesired primer dimers. Quantification was normalized using mouse β-actin as a reference gene. Expression levels of the specific genes were indicated as fold-changes compared with controls. Each assay was performed in triplicate.

Flow cytometric analysis

Fluorescence-labeled monoclonal antibodies, fluorescein isothiocyanate (FITC)-anti-CD24, phycoerythrin (PE)-anti-CD44, PE-anti-CD49f, and isotype-matched IgG controls were purchased from eBioscience (San Diego, CA). PE-anti-epithelial cell adhesion molecule (EpCAM) antibody was purchased from Miltenyi Biotec (Bergisch Gladbach, Germany). Flow cytometric analysis was performed using a flow cytometer (Cytomics FC500; Beckman Coulter, Fullerton, CA). Data were analyzed using FlowJo software (Tree Star, Ashland, OR).

Animal experiments

Intracardiac and intramammary injections of tumor cells into C57BL/6 mice (female, 8-week-old, Japan SLC, Shizuoka, Japan) were conducted as previously described [15, 16]. The number of mice used in each experiment is described in the figure legends. Body weight (BW) change was calculated by the following equation: % BW change = (BW on the specified day − BW on day 0)/BW on day 0 × 100. Mammary tumor volume was estimated by the following equation: Tumor volume (mm^3) = (length) × $(width)^2 \times 0.5$. All animal experiments were approved by the Animal Management Committee of Matsumoto Dental University.

Establishment of a highly bone-metastatic clone

A bone-metastatic clone of E0771 cells was established as previously described [13]. Two weeks after the intracardiac inoculation of parental E0771 cells, mice were killed and the cells in the bone marrow cavity were flushed out and cultured in growth medium. After 1–2 weeks of culture, obtained cancer cells were reinoculated into the left cardiac ventricle of 8-week-old, female, C57BL/6 mice. This procedure was repeated 15 times and a highly bone-metastatic clone was obtained.

Radiographic analysis of bone metastases

Development of bone metastases was monitored by X-ray radiography. Mice were anesthetized with pentobarbital (0.05 mg/g body weight; Kyoritsu Seiyaku, Tokyo, Japan), arranged in a prone position on single-wrapped films (Carestream Kodak BioMax XAR Film, Sigma-Aldrich), and exposed to a 20 kV X-ray at 3 mA for 8 s using a soft X-ray inverter system (SRO-iM50; Sofron, Tokyo, Japan).

Micro-computed tomography (μCT) analysis

The undecalcified femurs were subjected to μCT analysis using micro focus X-ray computed tomography (ScanXmate-A080; Comscantecno, Yokohama, Japan). Three-dimensional (3D) digital images were reconstructed using TRI/3D-BON software (Ratoc System Engineering, Tokyo, Japan).

Histologic and histomorphometric analysis

Paraffin sections were prepared by conventional methods and were stained with hematoxylin and eosin (H–E). Tartrate-resistant acid phosphatase (TRAP) staining was also performed as previously described [16]. Using H–E-stained sections, the presence or absence of metastases in 2 femurs and 2 tibias was evaluated under a microscope. Data are expressed as the number of bones with metastases/mouse. The metastases in adrenal glands, ovaries, and brains were also similarly evaluated. Histomorphometric analysis was conducted on the tumor burden in bones as previously described [15, 16]. Data are expressed as the tumor area (mm^2).

Measurement of serum calcium levels

Blood was collected from mice by cardiac puncture at the time of sacrifice. Serum calcium levels were measured using a kit (Calcium *E* test Wako, Wako Pure Chemical Industries, Osaka, Japan) according to the manufacturer's protocol.

Statistical analysis

Data are expressed as the mean ± SEM. Significance was analyzed by the Student's *t* test or Welch's *t* test (Mini Stat-Mate; ATMS, Tokyo, Japan). One-way ANOVA followed by the Tukey test was used when more than two groups were compared. *P* values of < 0.05 were considered to be significant.

Results

Establishment of a highly bone-metastatic clone of E0771 mouse breast cancer cells

We firstly evaluated the bone-metastatic ability of parental E0771 cells (E0771/Pa) and the bone-metastatic clone (E0771/Bone), which was established by 15-times-repeated in vivo sequential selection. Histological examination revealed that 20 of 23 (87%) and 19 of 19 (100%) mice intracardially inoculated, respectively, with E0771/Pa and E0771/Bone developed at least one metastatic lesion in femurs or tibias in C57BL/6 mice (data not shown). Of note, E0771/Bone developed significantly larger metastases with higher frequency than E0771/Pa (Fig. 1a, b). Both cells induced an essentially similar histological type of bone metastasis. The metastases were mainly osteolytic, which were recognized as radiolucent lesions on X-ray images (Fig. 1c). The majority of trabecular bones were destroyed and cortical bones were also penetrated in some parts (Fig. 1a, d). Many TRAP-positive multinucleated osteoclasts and mononucleated osteoclast precursor cells were seen on residual bone surfaces and in tumor nests (Fig. 1e). However, some trabecular bones remained undestroyed in the metastatic lesions (Fig. 1a, d).

The intracardiac inoculation of E0771/Pa cells also caused macroscopically detectable metastases in the adrenal glands and the ovaries in most mice (Fig. 2a, b). The frequency of the metastases was not decreased and even increased when inoculated with E0771/Bone (Fig. 2a, b). Moreover, brain metastases were found in 4 of 11 (36%)

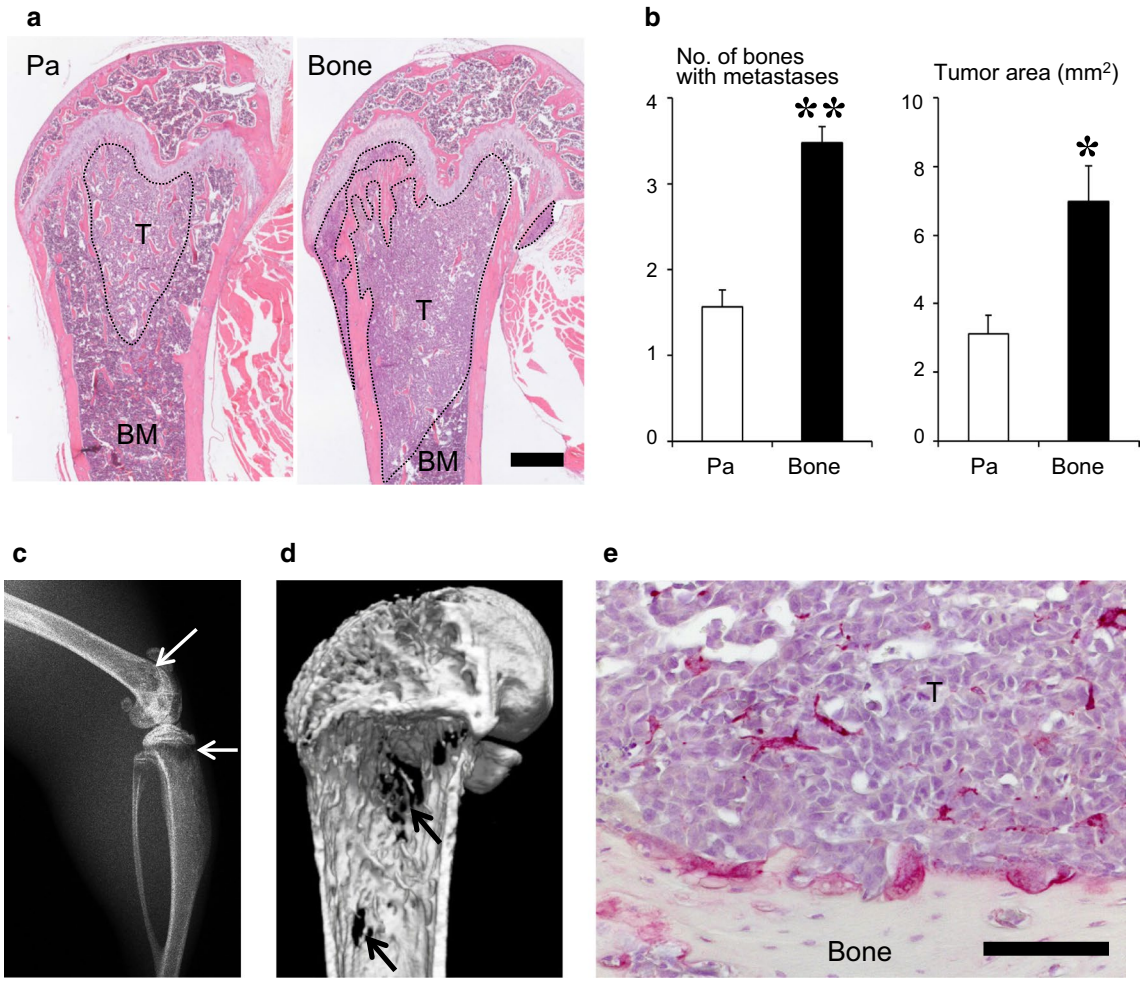

Fig. 1 Bone-metastatic potential of E0771/Pa (Pa) and E0771/Bone (Bone) in C57BL/6 mice. **a** Representative histologic views of metastases in the femurs at 2 weeks after intracardiac injection (H–E staining; *T* tumor; *BM* bone marrow; scale bar = 500 μm). The metastatic lesions are encircled with the dotted line. **b** Histologic and histomorphometric analysis of tumor burden of E0771/Pa and E0771/Bone in bone. Data are expressed as the number of bones with metastases (left) and the tumor area (mm^2, right) ($n = 23$ for E0771/Pa and $n = 19$ for E0771/Bone, combination of three separate experiments). $^*p < 0.01$; $^{**}p < 0.001$. **c** Representative X-ray image of bone metastases of E0771/Bone (arrows, radiolucent lesions). **d** Representative 3D μCT image of bone metastases of E0771/Bone. Some parts of the cortical bone were penetrated by the tumor expansion (arrows). **e** Representative histologic views of bone metastases of E0771/Bone stained with TRAP (*T* tumor; scale bar = 100 μm)

mice inoculated with E0771/Pa and 9 of 9 (100%) mice inoculated with E0771/Bone (Fig. 2c). No metastases were found in other organs by macroscopic examination. Tumor-bearing mice showed a time-dependent loss of body weight, which was more severe in E0771/Bone-inoculated mice (Fig. 2d), and started to die around 2 weeks after cell inoculation. No mice presented hypercalcemia at 2 weeks after intracardiac injection (data not shown).

Phenotypic differences between E0771/Pa and E0771/Bone

We then compared phenotypic differences between E0771/Pa and E0771/Bone in vitro. Both cells showed a similar spindle-like shape in monolayer cultures; however, E0771/Bone exhibited a relatively more uniform morphology (Fig. 3a). Cell proliferation in monolayer cultures was similar between E0771/Pa and E0771/Bone (Fig. 3b). Conventional RT-PCR analysis demonstrated that E0771/Pa was positive for ERα and Erbb2 (also known as HER2), but negative for PgR (Fig. 3c). E0771/Pa also expressed PTHrP mRNA. In E0771/Bone, the expression of PgR and Erbb2 was similar to E0771/Pa, while the expression of ERα was decreased and that of PTHrP was increased (Fig. 3c), which was confirmed by quantitative real-time PCR (Fig. 3d). The expression of PTHrP in E0771/Bone was enhanced by TGFβ, a growth factor abundantly stored

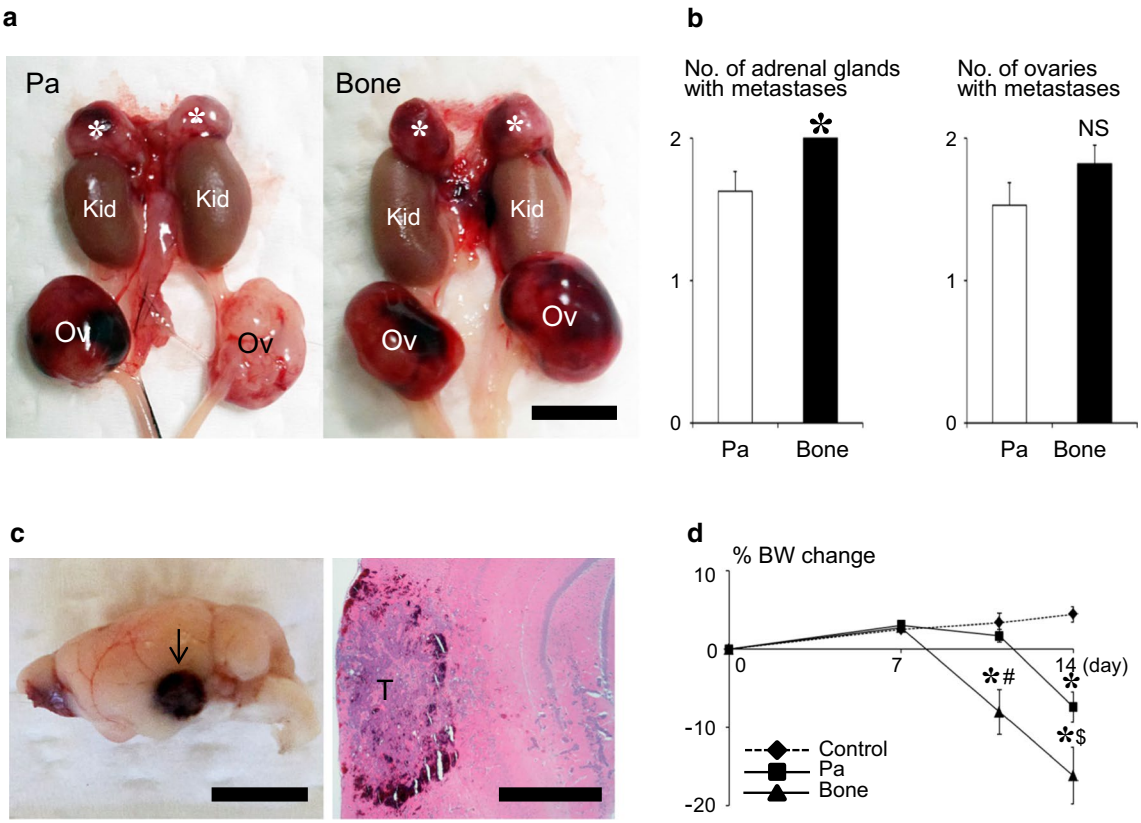

Fig. 2 Metastases of E0771/Pa (Pa) and E0771/Bone (Bone) to non-bone organs. **a** Representative macroscopic view of metastases in the adrenal glands (asterisk) and the ovaries (Ov) at 2 weeks after intracardiac injection (*Kid* kidney; scale bar = 5 mm). **b** Quantitative analysis of metastases in the adrenal glands and the ovaries. Data are expressed as the number of adrenal glands (left) or ovaries (right) with metastases ($n=23$ for E0771/Pa and $n=19$ for E0771/Bone, combination of three separate experiments). *$p<0.05$; *NS* not significant. **c** Representative macroscopic (left, arrow) and histological (right) view of metastases in the brain at 2 weeks after intracardiac injection of E0771/Bone (*T* tumor; scale bars = 5 mm in left panel and 1 mm in right panel). **d** BW changes in tumor-inoculated mice. Data are expressed as % BW change [$n=11$ for control (non-tumor-bearing mice) and E0771/Pa and $n=9$ for E0771/Bone]. *$p<0.001$ vs. control; $^{\#}p<0.01$ vs. E0771/Pa; $^{\$}p<0.05$ vs. E0771/Pa

in bone matrix, although the induction in E0771/Pa was not statistically significant (Fig. 3d).

Cancer stem-like properties of E0771/Bone

To clarify the mechanism of the enhanced metastatic capacity of E0771/Bone, the cancer stem-like properties were investigated. Suspension culture experiments showed that E0771/Bone formed significantly more tumorspheres than E0771/Pa (Fig. 4a). Furthermore, tumor growth in the orthotopic mammary fat pad was also facilitated to a greater extent in mice injected with E0771/Bone than in those injected with E0771/Pa (Fig. 4b). Then, we finally compared the expression of breast cancer stem-like markers. Flow cytometric analysis revealed that both E0771/Pa and E0771/Bone were CD24-negative and CD44-positive [17]; however, the expression was relatively more homogeneous and CD44 expression was slightly increased in E0771/Bone compared with E0771/Pa (Fig. 4c). The expression of CD49f [18] was also somewhat higher in E0771/Bone, whereas EpCAM [17] was negative in E0771/Pa and E0771/Bone (Fig. 4c). Real-time PCR analysis showed that the mRNA expression of BMI1 [19] was similar and that of ALDH1A1 [20] was at undetectable level in both cells (data not shown).

Discussion

In the current study, we established a novel C57BL/6 mouse model of bone metastases of breast cancer, which is one of the most common cancers to metastasize to bone [3]. To date, there have only been a few reports on the study of bone metastasis of breast cancer using C57BL/6 mice, because of limited available syngeneic cell lines. These studies employed cell lines, Py8119 [7] and PyMT-BO1 [8], obtained from spontaneously arising tumors in mouse mammary tumor virus promoter-driven Polyoma middle T-antigen (MMTV-PyMT) transgenic C57BL/6 mice. Both

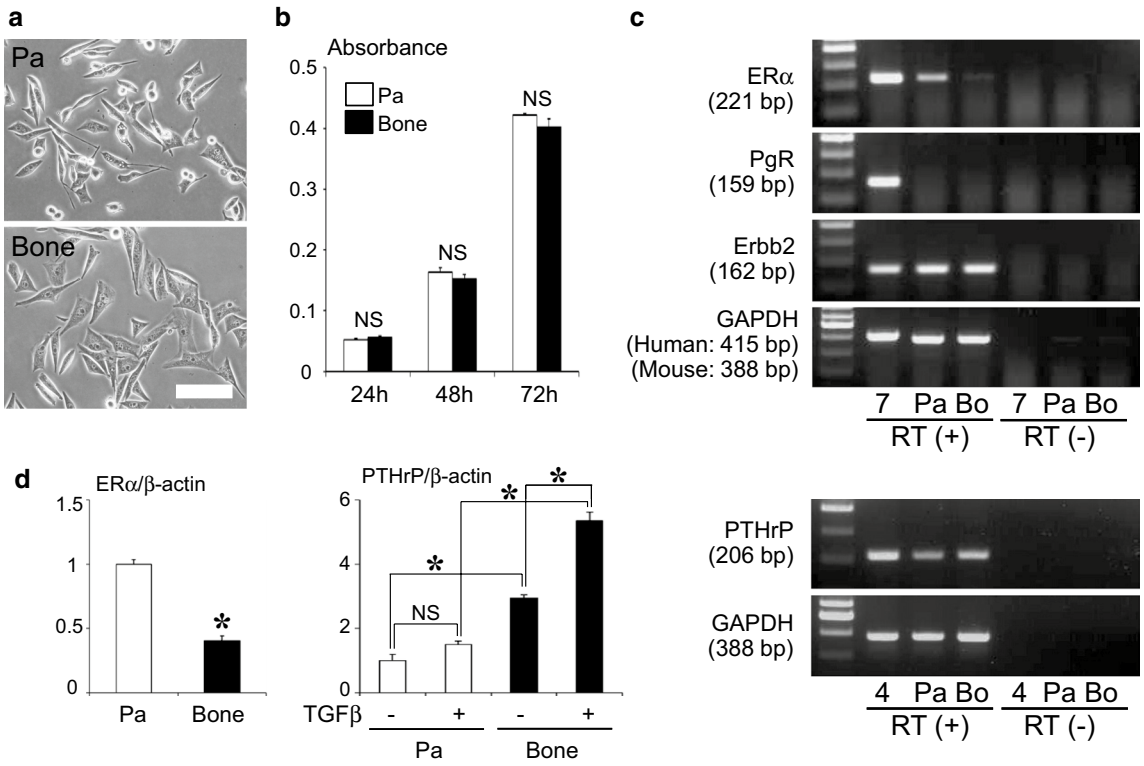

Fig. 3 Characterization of E0771/Pa (Pa) and E0771/Bone (Bone or Bo) in vitro. **a** Representative phase-contrast microscopy images in monolayer cultures (scale bar = 100 μm). **b** Cell proliferation in monolayer cultures determined by WST-8-based assay. Data are expressed as the absorbance at 450 nm. *NS* not significant. **c** mRNA expression of ERα, PgR, Erbb2, and PTHrP determined by conventional RT-PCR (30 cycles for ERα, PgR, Erbb2, and PTHrP, and 23 cycles for GAPDH). The primers for ERα, PgR, and Erbb2 amplify both mouse and human genes and the product sizes are the same. MCF-7 (7) and 4T1 (4) cells were used as positive controls. **d** Relative mRNA expression of ERα and PTHrP as determined by quantitative real-time RT-PCR. The treatment with TGFβ (5 ng/ml) was conducted for 24 h. Data are expressed as fold-changes compared to E0771/Pa. $^*p < 0.001$; *NS* not significant

Py8119 and PyMT-BO1 cells were shown to metastasize to bone after intracardiac inoculation; however, the incidence of bone metastases was low [7] or unclear [8]. On the other hand, the present study showed that most mice inoculated with E0771/Pa and E0771/Bone developed bone metastases (87 and 100%, respectively) within 2 weeks. Models using C57BL/6 mice have some advantages over models using other animals. Most importantly, C57BL/6 is the strain of mouse that is most frequently used for generating genetically engineered mice [4]. These mice enable us to investigate the influences of host environments on the development of bone metastases of breast cancer. Furthermore, since C57BL/6 mice are immunocompetent, these models can also be used to study the roles of the immune system in bone metastases of breast cancer.

The in vivo selection method employed in this study is a well-recognized and widely used method for isolating highly metastatic subpopulations from the parental populations [12]. Using this procedure, we previously established a highly bone-metastatic clone of MDA-MB-231 human breast cancer cells (MDA-231BO) [13]. Intracardiac inoculation of parental MDA-MB-231 cells developed metastases not only in bone, but also in non-bone organs, such as adrenal glands, ovaries, and the brain. In contrast, MDA-231BO exclusively metastasized to bone with larger lesions than the parental cells, suggesting that the in vivo selection enriched a bone-seeking population. However, in the present study, E0771/Bone acquired an enhanced metastatic potential to bone without losing that to adrenal glands, ovaries, and brain. These results suggest that, at least in this particular case, the in vivo selection yielded a more aggressive population, but not a bone-seeking population, likely through the enrichment of a population with cancer stem-like phenotypes.

The metastases of E0771/Pa and E0771/Bone induced mainly osteolytic changes in bone. However, when metastases were relatively small, bone destruction was not evident and the lesions partially exhibited the intertrabecular type [21] rather than the osteolytic type of bone metastases (Fig. 1a, E0771/Pa). Even when the lesions became large enough to destroy cortical bones, some trabecular bones still remained undestroyed (Fig. 1a, E0771/Bone). Accordingly, the lesions were somewhat difficult to distinguish on X-ray

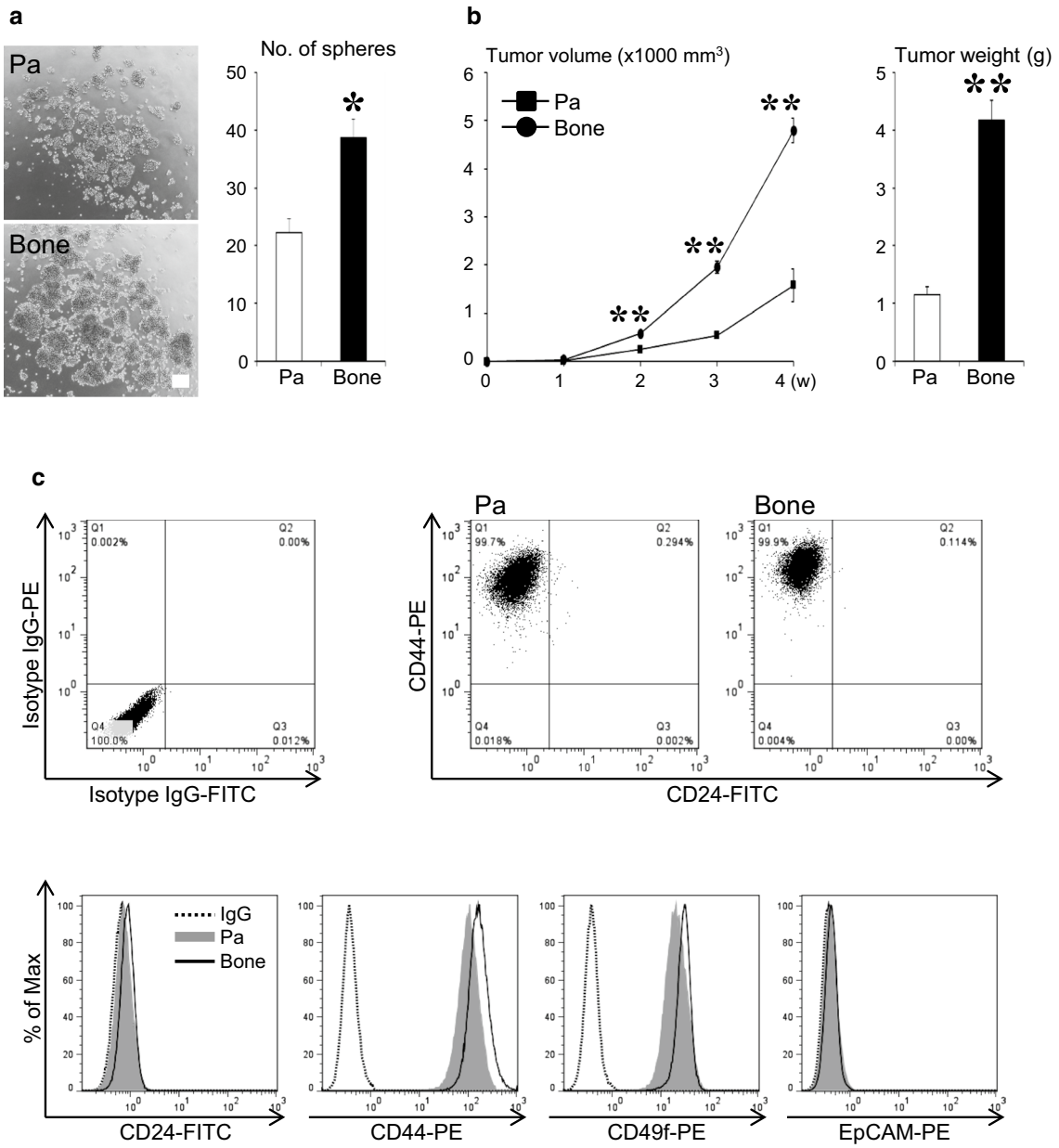

Fig. 4 Cancer stem-like properties of E0771/Bone. **a** Tumorsphere formation of E0771/Pa (Pa) and E0771/Bone (Bone) in suspension cultures. Representative microscopic images are shown on the left (scale bar = 200 μm). Quantitative data are expressed as the number of tumorspheres/well. $*p<0.01$. **b** Tumor growth in the orthotopic mammary fat pad of C57BL/6 mice. Data are expressed as the tumor volume (mm^3, left) and the tumor weight at the time of sacrifice at 4 weeks after cell inoculation (g, right) ($n=21$/group, combination of three separate experiments). $**p<0.001$. **c** Flow cytometric analysis of the expression of CD24, CD44, CD49f, and EpCAM. As controls, E0771/Pa was stained with isotype-matched IgGs

pictures (Fig. 1c) compared with pure osteolytic lesions caused by cancer cells such as MDA-MB-231 human breast cancer cells [22] and A375 human melanoma cells [23].

To determine the mechanisms of the enhanced metastatic potential of E0771/Bone, the phenotypical differences between E0771/Pa and E0771/Bone were examined in vitro and in vivo. Although cell morphology and proliferation in monolayer cultures showed no apparent differences, E0771/Bone exhibited increased tumorsphere formation in suspension cultures and tumor formation in the orthotopic mammary fat pad in C57BL/6 mice. Furthermore, E0771/Bone homogeneously expressed $CD24^{-}/CD44^{+}$, widely recognized markers of cancer stem-like cells of breast cancer [17], and CD44 expression was increased compared with E0771/Pa. These findings suggest that E0771/Bone possesses cancer stem-like properties. It has been well-described that

osteoclastic bone destruction plays a key role in the development of bone metastases [24]. PTHrP produced by cancer cells is one of the most common mediators of osteolytic bone metastases of breast cancer [25]. Quantitative RT-PCR analysis revealed that mRNA expression of PTHrP in E0771/Bone was higher than in E0771/Pa. Moreover, TGFβ, which is a growth factor abundantly stored in bone matrix and has been shown to increase the expression and production of PTHrP [26], significantly enhanced PTHrP expression only in E0771/Bone. The result suggests that E0771/Bone produces PTHrP more efficiently than E0771/Pa, especially in the bone microenvironment. Taken together, cancer stem-like properties and elevated PTHrP expression likely contribute to the enhanced metastatic potential of E0771/Bone.

In conclusion, we developed a novel C57BL/6 mouse model of bone metastases using the C57BL/6-derived breast cancer cell line E0771. We believe that our mouse model is a useful tool for in vivo studies of bone metastases of breast cancer, especially for those using genetically engineered mice with a C57BL/6 background.

Acknowledgements This work was supported in part by grants from JSPS KAKENHI (Grant number 15K11093), Japan.

Compliance with ethical standards

Conflict of interest All authors have no conflicts of interest.

References

1. The Editorial Board of the Cancer Statistics in Japan (2017) Cancer statistics in Japan 2016. Foundation for Promotion of Cancer Research, Tokyo
2. Siegel RL, Miller KD, Jemal A (2017) Cancer statistics, 2017. CA Cancer J Clin 67:7–30
3. Coleman RE (2006) Clinical features of metastatic bone disease and risk of skeletal morbidity. Clin Cancer Res 12:6243s–6249s
4. Rivera J, Tessarollo L (2008) Genetic background and the dilemma of translating mouse studies to humans. Immunity 28:1–4
5. Arguello F, Baggs RB, Frantz CN (1988) A murine model of experimental metastasis to bone and bone marrow. Cancer Res 48:6876–6881
6. Wakabayashi H, Wakisaka S, Hiraga T, Hata K, Nishimura R, Tominaga M, Yoneda T (2017) Decreased sensory nerve excitation and bone pain associated with mouse Lewis lung cancer in TRPV1-deficient mice. J Bone Miner Metab. https://doi.org/10.1007/s00774-017-0842-7
7. Biswas T, Gu X, Yang J, Ellies LG, Sun L-Z (2014) Attenuation of TGF-β signaling supports tumor progression of a mesenchymal-like mammary tumor cell line in a syngeneic murine model. Cancer Lett 346:129–138
8. Su X, Esser AK, Amend SR, Xiang J, Xu Y, Ross MH, Fox GC, Kobayashi T, Steri V, Roomp K, Fontana F, Hurchla MA, Knolhoff BL, Meyer MA, Morgan EA, Tomasson JC, Novack JS, Zou W, Faccio R, Novack DV, Robinson SD, Teitelbaum SL, DeNardo DG, Schneider JG, Weilbaecher KN (2016) Antagonizing integrin β3 increases immunosuppression in cancer. Cancer Res 76:3484–3495
9. Dunham LJ, Stewart HL (1953) A survey of transplantable and transmissible animal tumors. J Natl Cancer Inst 13:1299–1377
10. Ewens A, Mihich E, Ehrke MJ (2005) Distant metastasis from subcutaneously grown E0771 medullary breast adenocarcinoma. Anticancer Res 25:3905–3915
11. Mittal D, Sinha D, Barkauskas D, Young A, Kalimutho M, Stannard K, Caramia F, Haibe-Kains B, Stagg J, Khanna KK, Loi S, Smyth MJ (2016) Adenosine 2B receptor expression on cancer cells promotes metastasis. Cancer Res 76:4372–4382
12. Fidler IJ (1973) Selection of successive tumour lines for metastasis. Nat New Biol 242:148–149
13. Yoneda T, Williams PJ, Hiraga T, Niewolna M, Nishimura R (2001) A bone-seeking clone exhibits different biological properties from the MDA-MB-231 parental human breast cancer cells and a brain-seeking clone in vivo and in vitro. J Bone Miner Res 16:1486–1495
14. Aslakson CJ, Miller FR (1992) Selective events in the metastatic process defined by analysis of the sequential dissemination of subpopulations of a mouse mammary tumor. Cancer Res 52:1399–1405
15. Hiraga T, Ito S, Nakamura H (2011) Side population in MDA-MB-231 human breast cancer cells exhibits cancer stem cell-like properties without higher bone-metastatic potential. Oncol Rep 25:289–296
16. Hiraga T, Ito S, Nakamura H (2013) Cancer stem-like cell marker CD44 promotes bone metastases by enhancing tumorigenicity, cell motility, and hyaluronan production. Cancer Res 73:4112–4122
17. Al-Hajj M, Wicha MS, Benito-Hernandez A, Morrison SJ, Clarke MF (2003) Prospective identification of tumorigenic breast cancer cells. Proc Natl Acad Sci USA 100:3983–3988
18. Cariati M, Naderi A, Brown JP, Smalley MJ, Pinder SE, Caldas C, Purushotham AD (2008) Alpha-6 integrin is necessary for the tumourigenicity of a stem cell-like subpopulation within the MCF7 breast cancer cell line. Int J Cancer 122:298–304
19. Liu S, Dontu G, Mantle ID, Patel S, Ahn NS, Jackson KW, Suri P, Wicha MS (2006) Hedgehog signaling and Bmi-1 regulate self-renewal of normal and malignant human mammary stem cells. Cancer Res 66:6063–6071
20. Tomita H, Tanaka K, Tanaka T, Hara A (2016) Aldehyde dehydrogenase 1A1 in stem cells and cancer. Oncotarget 7:11018–11032
21. Yamaguchi T, Tamai K, Yamato M, Honma K, Ueda Y, Saotome K (1996) Intertrabecular pattern of tumors metastatic to bone. Cancer 78:1388–1394
22. Hiraga T, Williams PJ, Mundy GR, Yoneda T (2001) The bisphosphonate ibandronate promotes apoptosis in MDA-MB-231 human breast cancer cells in bone metastases. Cancer Res 61:4418–4424
23. Hiraga T, Nakajima T, Ozawa H (1995) Bone resorption induced by a metastatic human melanoma cell line. Bone 16:349–356
24. Yoneda T, Hiraga T (2005) Crosstalk between cancer cells and bone microenvironment in bone metastasis. Biochem Biophys Res Commun 328:679–687
25. Guise TA, Yin JJ, Taylor SD, Kumagai Y, Dallas M, Boyce BF, Yoneda T, Mundy GR (1996) Evidence for a causal role of parathyroid hormone-related protein in the pathogenesis of human breast cancer-mediated osteolysis. J Clin Invest 98:1544–1549
26. Yin JJ, Selander K, Chirgwin JM, Dallas M, Grubbs BG, Wieser R, Massagué J, Mundy GR, Guise TA (1999) TGF-beta signaling blockade inhibits PTHrP secretion by breast cancer cells and bone metastases development. J Clin Invest 103:197–206